

## Supplementary Materials

### Tables

Table S1. Cell parameters of FSO and FSOH obtained by XRD refinement.

Samples	<i>a</i>	<i>b</i>	<i>c</i>	V(Å <sup>3</sup> )
FSO	6.4222	12.6161	13.1916	1068.8229
FSOH	9.3457	9.3457	20.2222	1529.6171

Table S2. The Raman tensors R for Raman-active modes in FSOH.

<i>R</i>	$R(A_1) = \begin{pmatrix} a & 0 & 0 \\ 0 & a & 0 \\ 0 & 0 & b \end{pmatrix}; R(E) = \begin{pmatrix} 0 & c & d \\ c & 0 & 0 \\ d & 0 & 0 \end{pmatrix}$
----------	--------------------------------------------------------------------------------------------------------------------------------------------------------

Table S3. The Raman intensity of A<sub>1</sub> and E modes in FSOH under different configurations.

<i>A</i>	// (XX)	$I \propto (a\cos^2 \theta + b\sin^2 \theta)^2$
	⊥ (XY)	$I \propto \left(\frac{b-a}{2}\sin 2\theta\right)^2$
<i>E</i> <sub>1</sub>	// (XX)	$I \propto (d\sin 2\theta)^2$
	⊥ (XY)	$I \propto (d \cos 2\theta)^2$

Table S4. The complex Raman tensor element with the imaginary part in FSOH.

$$R(A_1) = \begin{pmatrix} |a|e^{i\varphi_a} & 0 & 0 \\ 0 & |a|e^{i\varphi_a} & 0 \\ 0 & 0 & |b|e^{i\varphi_b} \end{pmatrix};$$

$$R(E) = \begin{pmatrix} 0 & |c|e^{i\varphi_c} & |d|e^{i\varphi_d} \\ |c|e^{i\varphi_c} & 0 & 0 \\ |d|e^{i\varphi_d} & 0 & 0 \end{pmatrix}$$

Table S5. The Raman intensity of A<sub>1</sub> and E modes in FSOH under different configurations.

	// (XX)	$I \propto a^2\cos^4 \theta + b^2\sin^4 \theta + \frac{1}{2} a  b \cos(\varphi_a - \varphi_b)$
--	---------	------------------------------------------------------------------------------------------------

	$\perp (XY)$	$I \propto \frac{1}{4} \sin^2 2\theta [a^2 + b^2 - 2 a  b \cos(\varphi_{a-b})]$ $)^2$
$E$	// (XX)	$I \propto ( d \sin 2\theta)^2$
	$\perp (XY)$	$I \propto ( d \cos 2\theta)^2$

Table S6. The complex Raman tensor element with the imaginary part in FSO.

$$R(A_g) = \begin{pmatrix} |a|e^{i\phi_a} & 0 & 0 \\ 0 & |b|e^{i\phi_b} & 0 \\ 0 & 0 & |c|e^{i\phi_c} \end{pmatrix};$$

$$R(B_{2g}) = \begin{pmatrix} 0 & 0 & |e|e^{i\phi_e} \\ 0 & 0 & 0 \\ |e|e^{i\phi_e} & 0 & 0 \end{pmatrix}$$

Table S7. The Raman intensity of  $A_g$  and  $B_{2g}$  modes in FSO.

$A_g$	// (XX)	$I \propto a^2 \cos^4 \theta + c^2 \sin^4 \theta + \frac{1}{2}  a  c \cos(\varphi_{a-t})$
	$\perp (XY)$	$I \propto \frac{1}{4} \sin^2 2\theta [a^2 + c^2 - 2 a  c \cos(\varphi_{a-b})]$ $)^2$
$B_{2g}$	// (XX)	$I \propto (es\sin 2\theta)^2$
	$\perp (XY)$	$I \propto (e \cos 2\theta)^2$

## Figures

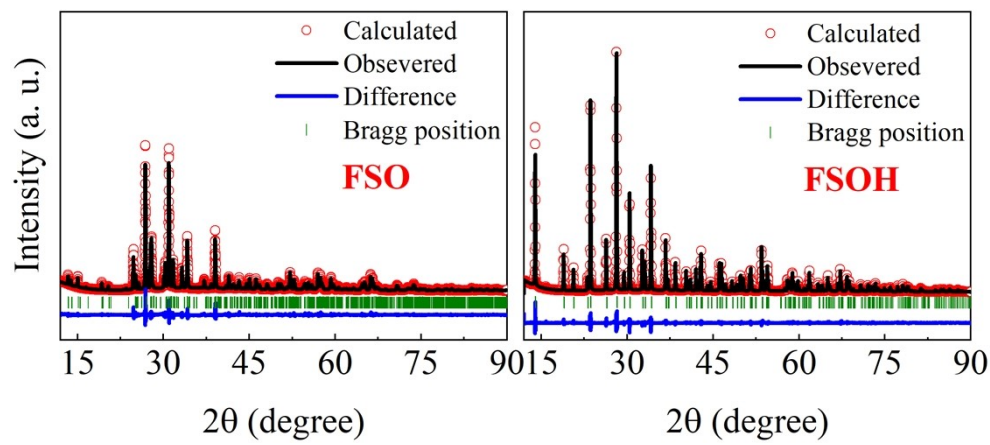


Fig. S1 Refined XRD mapping results of FSO and FSOH.

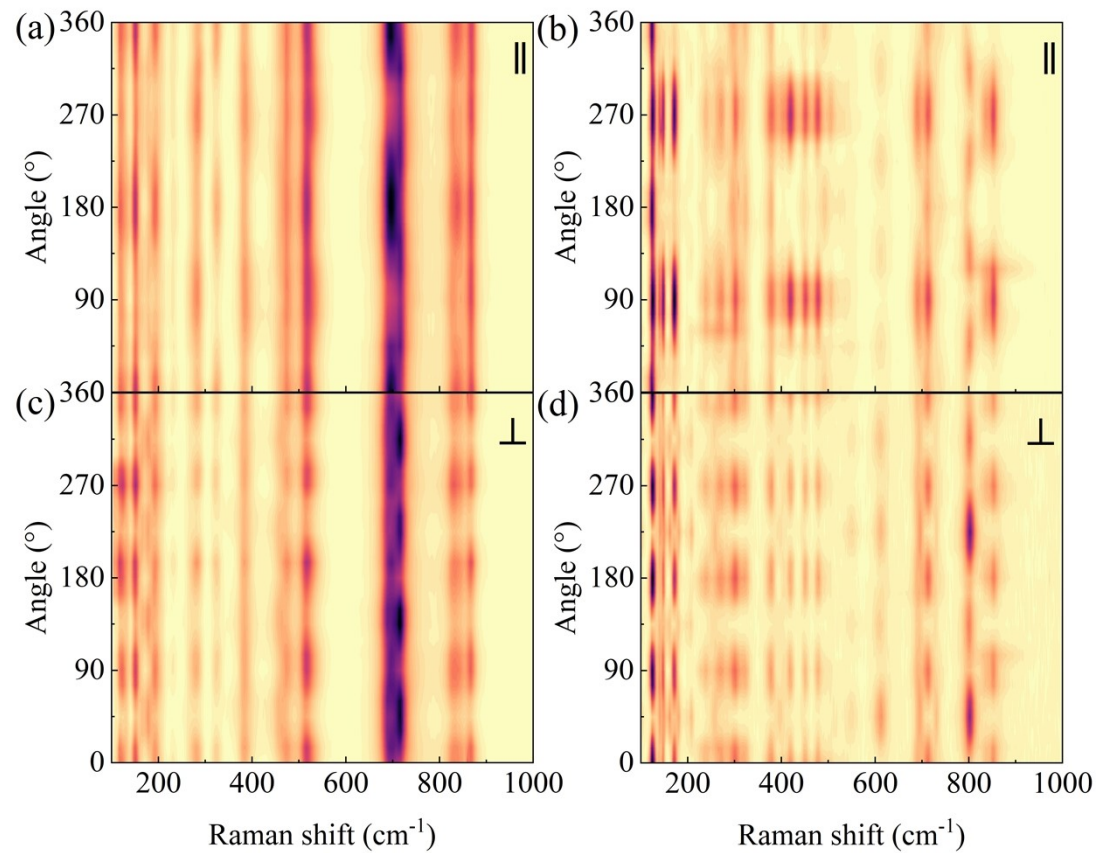
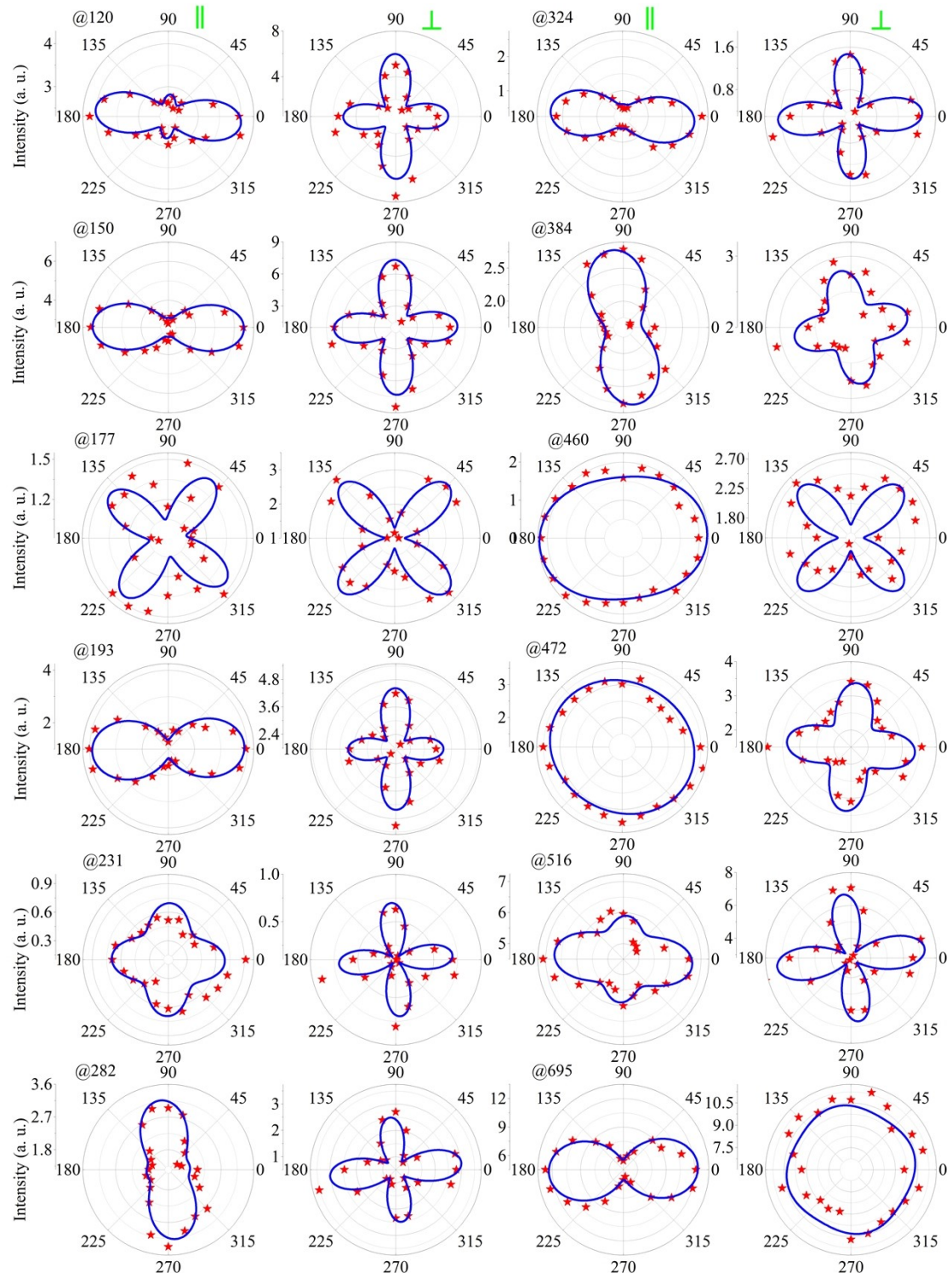


Fig. S2 The Raman intensity contour plots of FSOH (a, c) and FSO (b, d) under parallel and cross configurations.



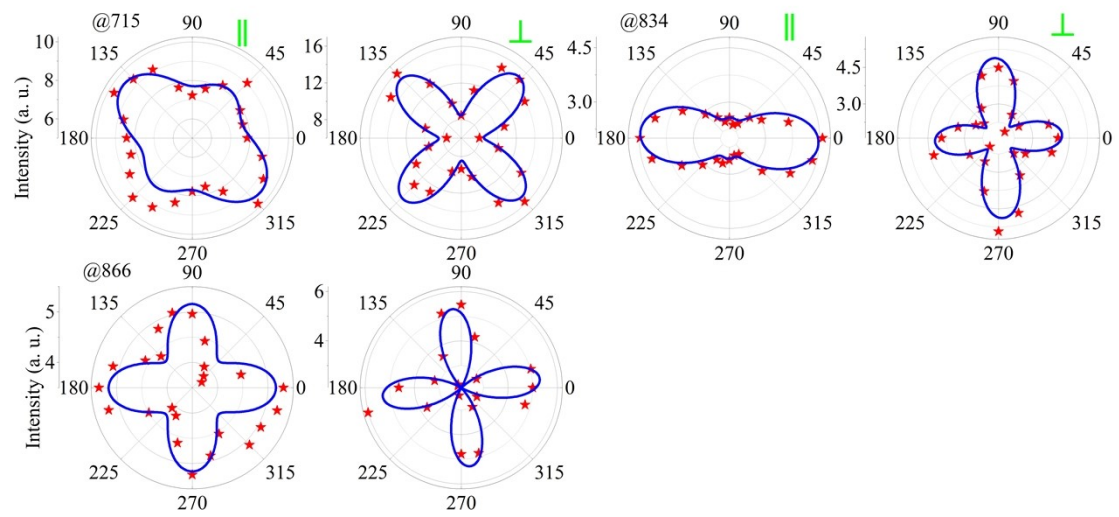
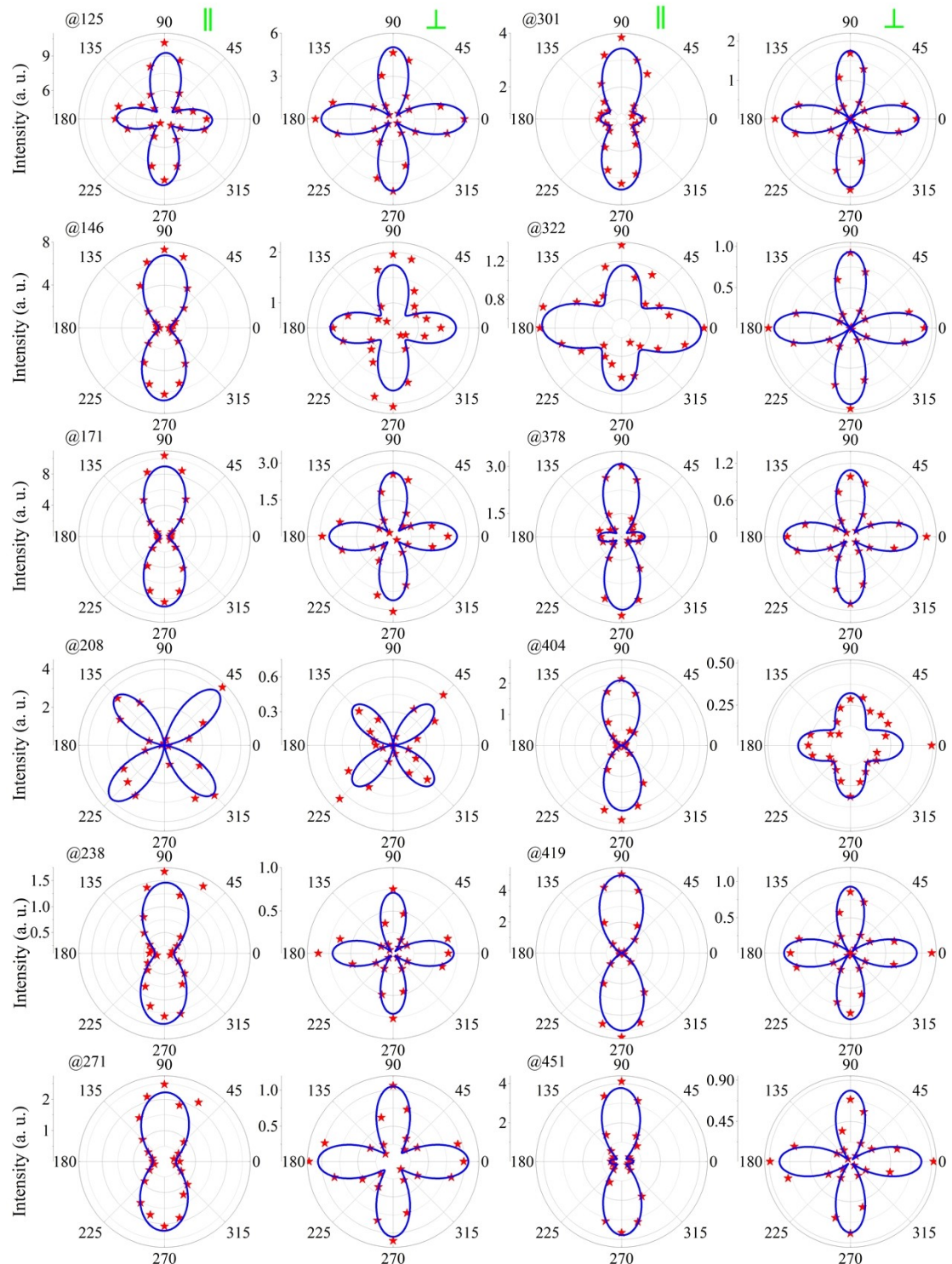


Fig. S3 Polar plot of the ARPRS results of FSOH under parallel and cross configurations.



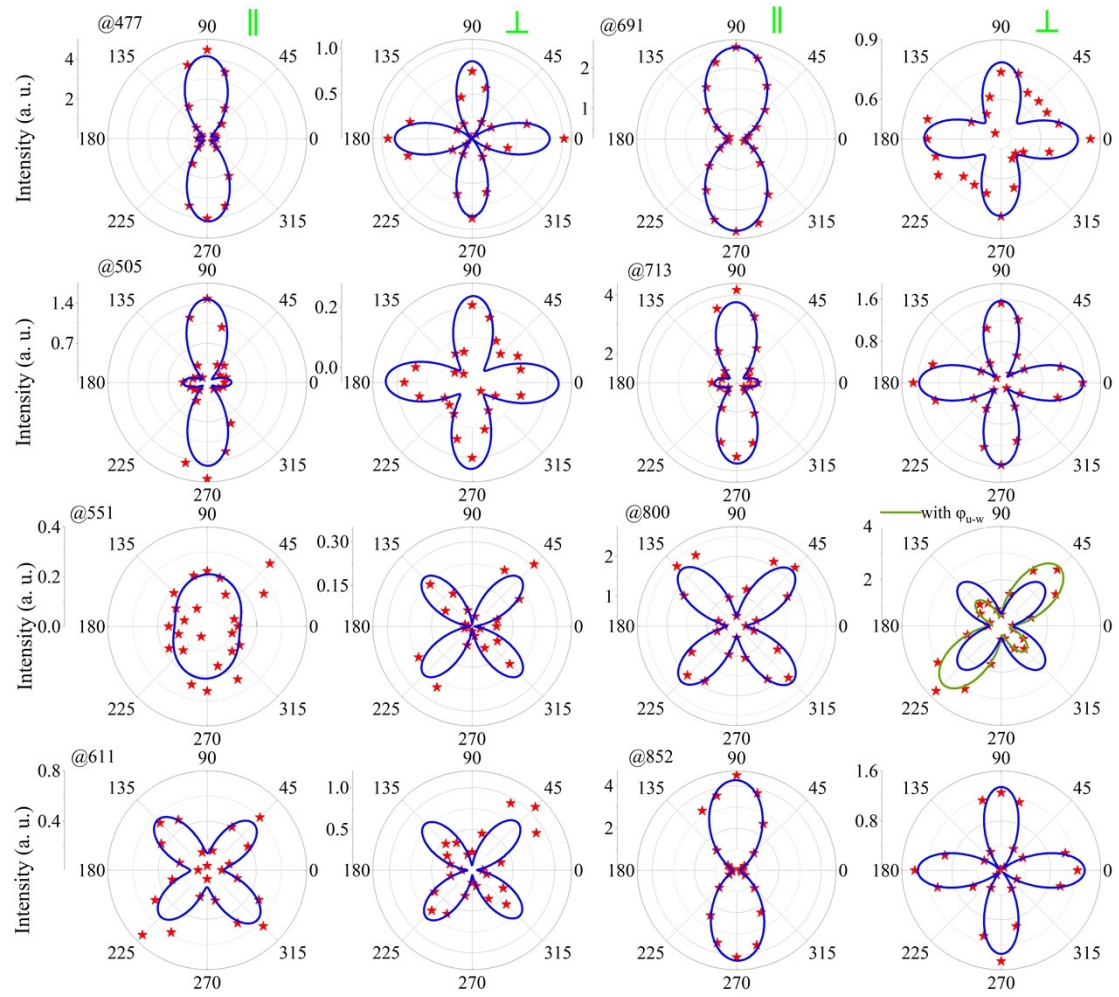


Fig. S4 Polar plots of the ARPRS results of FSO under parallel and cross configurations.